Chemical Science

EDGE ARTICLE

View Article Online
View Journal | View Issue

Check for updates

Cite this: *Chem. Sci.*, 2018, **9**, 6210

Large-bite diboranes for the μ(1,2) complexation of hydrazine and cyanide†

Chang-Hong Chen and François P. Gabbaï*

As part of our interest in the chemistry of polydentate Lewis acids as hosts for diatomic molecules, we have investigated the synthesis and coordination chemistry of bidentate boranes that feature a large boron–boron separation. In this paper, we describe the synthesis of a new example of such a diborane, namely 1,8-bis(dimesitylboryl)triptycene (**2**) and compare its properties to those of the recently reported 1,8-bis(dimesitylboryl)biphenylene (**1**). These comparative studies reveal that these two diboranes feature some important differences. As indicated by cyclic voltammetry, **1** is more electron deficient than **2**; it also adopts a more compact and rigid structure with a boron–boron separation (4.566(5) Å) shorter by ~1 Å than that in **2** (5.559(4) Å). These differences appear to dictate the coordination behaviour of these two compounds. While **2** remains inert toward hydrazine, we observed that **1** forms a very stable μ(1,2) hydrazine complex which can also be obtained by phase transfer upon layering a solution of **1** with a dilute aqueous hydrazine solution. The stability of this complex is further reflected by its lack of reaction with benzaldehyde at room temperature. We have also investigated the behaviour of **1** and **2** toward anions. In MeOH/$CHCl_3$ (1/1 vol) both compounds selectively bind cyanide to form the corresponding μ(1,2) chelate complexes with a B–C≡N–B bridge at their cores. Competition experiments in protic media show that the anionic cyanide complex formed by **1** is the most stable, with no evidence of decomplexation even in the presence of $(C_6F_5)_3B$.

Received 24th April 2018
Accepted 27th May 2018

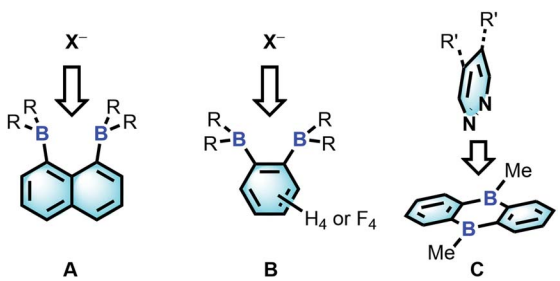
DOI: 10.1039/c8sc01877d

rsc.li/chemical-science

Open Access Article. Published on 29 May 2018. Downloaded on 3/28/2024 8:53:24 AM.
This article is licensed under a Creative Commons Attribution-NonCommercial 3.0 Unported Licence.

Introduction

The chemistry of main group-based polydentate Lewis acids[1] has drawn considerable attention over the past decades, leading to applications in anion sensing,[2] anion transport,[3] small molecule activation and catalysis.[4] Diboranes featuring the rigid 1,8-naphthalenediyl[5] or *ortho*-phenylene[6] backbones are the most studied examples of such systems. Owing to the short spacing of the two boron centres, these diboranes are well-suited for the chelation of monoatomic anions such as hydride,[5a,5b,6a] fluoride[5a,5e,5g,6a] and chloride[5c,6b] or polyatomic anions amenable to μ(1,1) ligation such as azide.[5g,6c] The strength of the diborane host-anionic guest interaction in these system has led to the development of application in selective anion sensing[5a–c,e,g,6a] as well as catalysis.[4g,5e,6b,c] Although no structural evidence has been obtained for the ditopic complexation of neutral molecules by diboranes of type **A** and **B**, it has been demonstrated recently that 9,10-dihydroanthracenes of type **C** are able to engage 1,2-diazines in complex formation[7] and catalyse their Diels Alder chemistry.[6g,8] The ability of **C** to complex 1,2-diazines is reminiscent of the adduct formed by 2,2′-diborabiphenyl and pyridazine.[9]



A X = H, F, Cl, N_3 **B** X = F, Cl, N_3 **C**

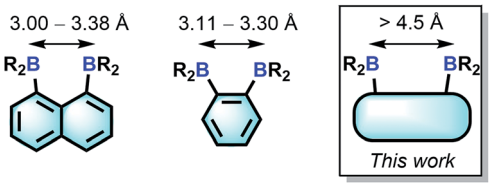
Bearing in mind that the selectivity of these diboranes for their respective guests is dictated by the size match that exists between the host and the guest, we have recently become interested in diboranes with an increased separation between the Lewis acidic centres.[10] It occurred to us that such systems may display a different selectivity and may become well adapted to the μ(1,2) chelation of diatomic molecules.[11] We also speculated that the rigidity of the targeted diboranes may inform the molecular recognition properties of these bidentate Lewis acidic hosts.

Department of Chemistry, Texas A&M University, College Station, Texas 77843-3255, USA. E-mail: francois@tamu.edu

† Electronic supplementary information (ESI) available: Experimental details, NMR spectra of novel compounds, crystallographic data, absorption and emission spectra, DFT optimization results. CCDC 1838442, 1827003–1827005. For ESI and crystallographic data in CIF or other electronic format see DOI: 10.1039/c8sc01877d

This journal is © The Royal Society of Chemistry 2018

Open Access Article. Published on 29 May 2018. Downloaded on 3/28/2024 8:53:24 AM.
This article is licensed under a Creative Commons Attribution-NonCommercial 3.0 Unported Licence.

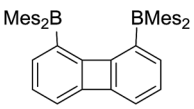


In this article, we report a series of results concerning the synthesis and properties of bidentate diboranes in which the two boron atoms are separated by more than 4.5 Å. We also show that this increased separation allows for the selective μ(1,2) complexation of hydrazine and cyanide, two diatomic molecules that are known for their high toxicity.

Results and discussion

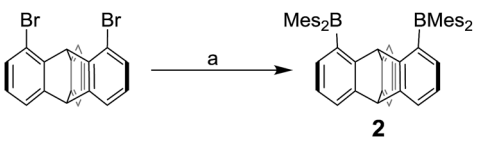
Synthesis, characterization and properties of the diboranes

We have recently described the synthesis of 1,8-bis(dimesitylboryl)biphenylene (**1**),[12] a diborane in which the two boron atoms are separated by 4.566(5) Å. To assess the influence of the backbone over the properties of such large-bite diboranes, we have now decided to prepare its 1,8-triptycenediyl analogue (**2**). By analogy with the approach we employed to access **1**, diborane **2** was obtained *via* the dilithiation of 1,8-dibromotriptycene, followed by metathesis with Mes_2BF (Scheme 1).



1

Compound **2** is a colourless air-stable solid which has been isolated in moderate yield. The ^{1}H NMR signals of the triptycene backbone are consistent with a symmetrical structure. The detection of six sharp signals arising from the methyl groups and the four *meta*-H signals of the mesityl groups suggest that the molecule retains mirror symmetry in solution. The ^{11}B NMR spectrum shows a broad peak at 73.0 ppm which falls within the typical range expected for triarylboranes. The cyclic voltammogram (CV) of compound **2** shows two quasi-reversible reduction waves at −2.62 and −3.00 V *vs.* Fc/Fc^+, suggesting that the molecule can be reduced by two electrons (Fig. 1c). Compared to the biphenylene derivative **1** for which the two reduction waves are observed at $E_{1/2}$ = −2.23 and −2.74 V (Fig. 1c),[12] the first reduction of **2** is shifted toward cathodic potentials by 390 mV. This observation indicates that the biphenylene backbone is substantially more electron withdrawing. This conclusion is in agreement with two previous studies dealing with related



2

Scheme 1 Synthesis of diborane **2**. (a) 2.3 equiv. ^{n}BuLi, 2.2 equiv. Mes_2BF, THF, −78 °C.

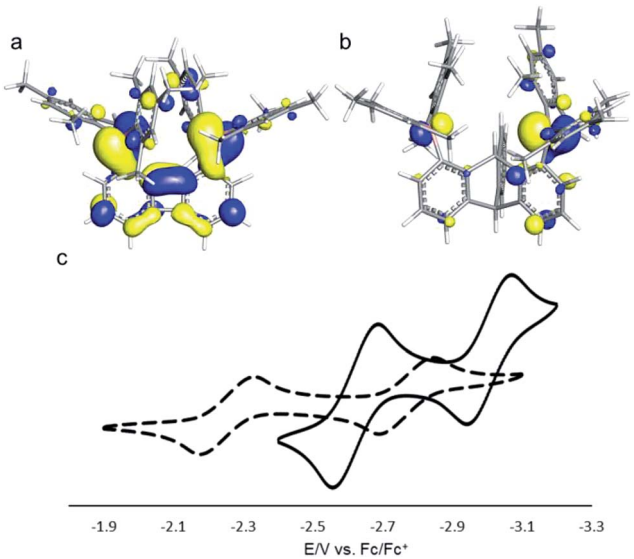


Fig. 1 (a) LUMO of **1** (isovalue = 0.03). (b) LUMO of **2** (isovalue = 0.05). (c) Cyclic voltammograms of **1** (dash line, $E_{1/2}$ = −2.23 and −2.74 V) and **2** (solid line, $E_{1/2}$ = −2.62 and −3.00 V) in THF. Scan rate = 100 mV s^{-1}.

biphenylene boron derivatives.[12,13] Also, the shorter separation observed between the first and second reduction wave in **2** ($\Delta E_{1/2}$ = 0.51 V for **1** *vs.* $\Delta E_{1/2}$ = 0.38 V for **2**) signals a decreased electronic communication between the boron atoms, an effect that we assign to the absence of extended conjugation in the triptycene backbone. The importance of electronic communication in **1** is further supported by the fact that the $\Delta E_{1/2}$ measured for **1** (0.51 V) is comparable to the largest value measured for naphthalene-based diboranes ($\Delta E_{1/2}$ range = 0.3–0.52 V), a class of compounds in which the two boron atoms are separated by only 3.002–3.385 Å.[5e,14]

Computational studies show that the lowest unoccupied molecular orbital (LUMO) of **1** (Fig. 1a) is dominated by the two boron p_π orbitals which are in conjugation with the biphenylene π system. The makeup of this LUMO underscores the effective electronic communication that exists between the two boron centres. In the case of **2**, which lacks mirror symmetry because of steric repulsions between the mesityl substituents, the LUMO bears a larger contribution from the p_π orbital of one boron atom. The LUMO + 1, which lies only 0.14 eV above the LUMO, shows a large contribution from the opposite boron atom (see ESI†). More importantly, π-conjugation between the two boron atoms in **2** is interrupted by the sp^3 triptycene bridgehead carbon atoms. These features corroborate the conclusion that the two boron atoms of **1** are in closer electronic communication than in **2**, as confirmed from the CV measurements.

Single crystals of compound **2** could be obtained by layering a solution of **2** in CH_2Cl_2 with MeOH. The solid-state structure of **2** shows that the boron atoms adopt a trigonal planar geometry as indicated by the sum of the C_{aryl}–B–C_{aryl} angles ($\sum\angle_{C-B1-C} = 359.7°$, $\sum\angle_{C-B2-C} = 359.4°$) (Fig. 2).[15] The B1–B2 separation of 5.559(4) Å in **2** is notably larger than that in **1**

Open Access Article. Published on 29 May 2018. Downloaded on 3/28/2024 8:53:24 AM.
This article is licensed under a Creative Commons Attribution-NonCommercial 3.0 Unported Licence.

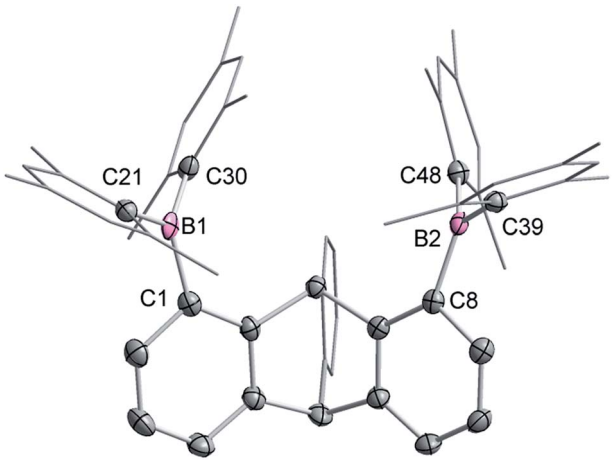


Fig. 2 Solid-state structure of **2**. Thermal ellipsoids are drawn at the 50% probability level. The hydrogen atoms are omitted for clarity. Selected bond lengths [Å] and angles [°]: B1–C1 1.564(4), B1–C21 1.518(3), B1–C30, 1.571(4), B2–C8 1.572(4), B2–C39 1.577(4), B2–C48 1.570(4); C1–B1–C21 117.5(2), C1–B1–C30 119.1(2), C21–B1–C30 123.1(2), C8–B2–C39 117.6(2), C8–B2–C48 121.1(2), C39–B2–C48 120.7(2).

(4.566(5) Å)[12] and 1,8-bis(diphenylboryl)naphthalene (3.002(2) Å).[14a] In $CHCl_3$/MeOH (1/1 vol), the UV-vis spectra of **1** and **2** feature a low-energy absorption band at 424 nm for **1** (Fig. 3) and 316 nm for **2** (Fig. 4). Time-dependent density functional theory (TD-DFT) calculations and Natural Transition Orbitals (NTO) analysis show the dominant HOMO–LUMO character of these transitions as observed for most triaryl boranes (see ESI†).[16] Both **1** and **2** are weakly fluorescent (QY = 0.05 for **1** and 0.04 for **2**) at a wavelength of 528 nm and 383 nm, respectively. Given that the boron orbitals are involved in the LUMO of both derivatives, it can be anticipated that the coordination of Lewis bases to the tricoordinate boron centres will dramatically affect these spectral features.[16e,17]

Reactions of the diboranes with neutral diatomic molecules

With **1** and **2** at our disposal, we became eager to investigate the behaviour of these two compounds in the presence of simple diatomic molecules including hydrogen peroxide, hydroxylamine and hydrazine. While complexes containing doubly

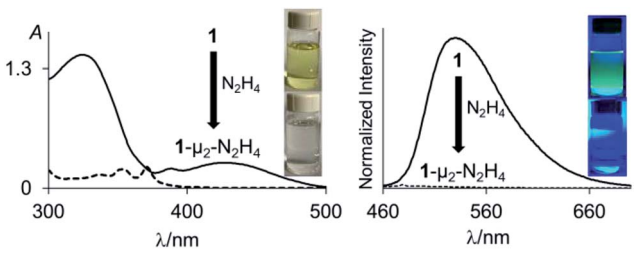


Fig. 3 UV-vis absorption (left) and emission (right) spectra of **1** (solid line) and **1**-μ_2-N_2H_4 (dash line) (4.52×10^{-5} M, $\lambda_{ex} = 370$ nm) in THF. The pictures of the solutions were taken at the same concentration. The images showing the fluorescence emission were illuminated with a hand-held UV lamp.

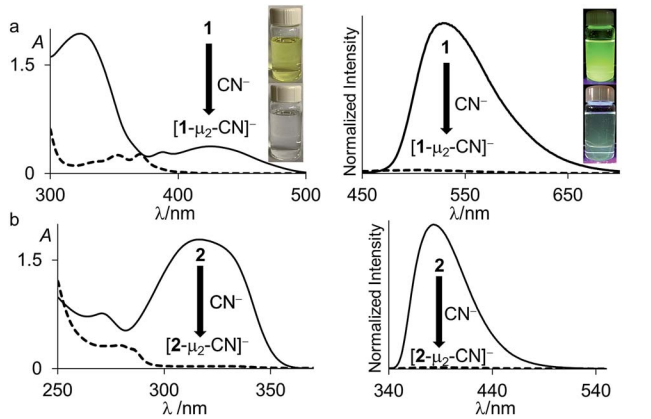
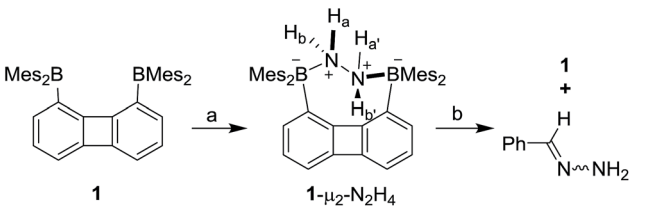


Fig. 4 UV-vis absorption (left) and emission (right) spectra of (a) **1** (solid line) and [**1**-μ_2-CN]$^-$ (dash line) (6.91×10^{-5} M, $\lambda_{ex} = 370$ nm) and (b) **2** (solid line) and [**2**-μ_2-CN]$^-$ (dash line) (6.22×10^{-5} M, $\lambda_{ex} = 280$ nm) in $CHCl_3$/MeOH (1/1 vol). The pictures of the solutions were taken at the same concentration. The images showing the fluorescence emission were illuminated with a hand-held UV lamp.

coordinated peroxide[11a,b] and hydrazine[18] molecules have generated much interest in the context of energy related research, we also note that coordinated hydrazine has been identified as a possible intermediate in nitrogen fixation reactions.[10c,19] Because of its acute toxicity, there are also numerous ongoing efforts aimed at developing selective receptors for molecular recognition and sensing applications.[20]

Inspired by the recent discovery that perfluorinated boranes can doubly complex the peroxide and superoxide anions,[21] we first tested the reaction of **1** and **2** with 30% $H_2O_{2(aq)}$. Unfortunately, we observed decomposition, illustrating the vulnerability of these non-perfluorinated diboranes under oxidative conditions. We also tested the reaction of **1** and **2** with 50% $NH_2OH_{(aq)}$, which also resulted in decomposition of the hosts. By contrast, reaction of diborane **1** with hydrazine monohydrate ($N_2H_4 \cdot H_2O$) in THF proceeded smoothly to afford the corresponding hydrazine complex **1**-μ_2-N_2H_4 as an air- and moisture-stable off-white solid (Scheme 2). This reaction results in a distinct loss of the yellow colour indicating coordination of the hydrazine to each boron atom. The same effect is responsible for the observed quenching of the green fluorescence (Fig. 3). In stark contrast, diborane **2** does not complex hydrazine under the same condition, even with a large excess of $N_2H_4 \cdot H_2O$. The lack of reactivity of **2** toward hydrazine may be correlated to its lower Lewis acidity as suggested by the CV measurements. It is also possible that the



Scheme 2 Synthesis of **1**-μ_2-N_2H_4 and the reaction of **1**-μ_2-N_2H_4 with benzaldehyde. (a) 2.5 equiv. $N_2H_4 \cdot H_2O$, THF, rt. (b) 1 equiv. benzaldehyde, $CDCl_3$, 60 °C.

This journal is © The Royal Society of Chemistry 2018

Open Access Article. Published on 29 May 2018. Downloaded on 3/28/2024 8:53:24 AM.
This article is licensed under a Creative Commons Attribution-NonCommercial 3.0 Unported Licence.

increased spacing between the two boron atoms, the lower rigidity of the backbone[22] and the presence of a bridgehead methine group interfere with the ability of **2** to bind hydrazine.

The ^{1}H NMR spectrum recorded for the resulting hydrazine adduct **1**-μ_2-N_2H_4 in CD_2Cl_2 features six methyl-proton and four *meta*-proton resonances, indicating that the complex adopts C_2 symmetry in solution. The most conspicuous evidence for the formation of a B–NH_2–NH_2–B bridge is the detection of two broad multiplets at 5.15 and 6.29 ppm, indicating that the B–NH_2–NH_2–B unit gives rise to an AA′BB′ spin system. These spectroscopic features also indicate that the conformation of the hydrazine molecule in the diboron pocket is rigidly locked in solution. The solid-state structure of **1**-μ_2-N_2H_4 offers a consistent picture (Fig. 5). This neutral complex crystallizes in the monoclinic *C*2/*c* space group with a half molecule in the asymmetric unit.[15] The hydrazine nitrogen atoms are coordinated to the boron atoms *via* a B–N bond length of 1.688(2) Å which is longer than that in H_3B–NH_2–NH_2–BH_3 (1.609 Å)[23] but comparable to that recently reported by Szymczak for complex **D**-μ_2-N_2H_4 (1.697(2) Å and 1.698(2) Å) (Scheme 3).[10c]

The N–N bond length of 1.469(2) Å is similar to the N–N bond length determined previously in the literature.[24] This observation clearly indicates that diborane **1** is well suited for the chelation of hydrazine molecule. We also note that **D** can bind two hydrazine molecules, one at each boron atom. This is not the case of diborane **1** which only forms a 1 : 1 complex, even in the presence of an excess of hydrazine. This difference in behaviour illustrates the selectivity imparted by the rigid preorganization of the two boron atoms in **1**.[10c]

To further establish the high affinity that **1** displays for hydrazine, we have studied the complexation reaction under dilute conditions. We observed that diborane **1** is capable of capturing hydrazine from dilute aqueous solutions under biphasic conditions. Quantitative formation of **1**-μ_2-N_2H_4 was observed by ^{1}H NMR spectrometry when a solution of **1** in CH_2Cl_2 (1 mL, [**1**] = 7.7 mM) was stirred for 24 hours with an aqueous solution (2.5 mL) containing 1 weight% of N_2H_4. Complex **1**-μ_2-N_2H_4 is remarkably stable. It can be stored in air and shows no evidence of decomposition for months. It is also resistant to reactions with aldehydes. For example, **1**-μ_2-N_2H_4 failed to react with benzaldehyde in $CDCl_3$ at room temperature over the course of 20 h. However, upon heating to 60 °C, a clean, yet slow reaction is observed leading to the quantitative formation of the free diborane **1** and benzaldehyde hydrazone after 20 h as confirmed by ^{1}H NMR spectroscopy (Scheme 2).[25]

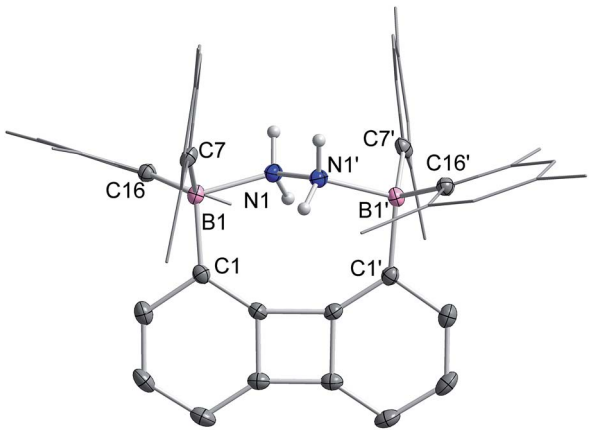
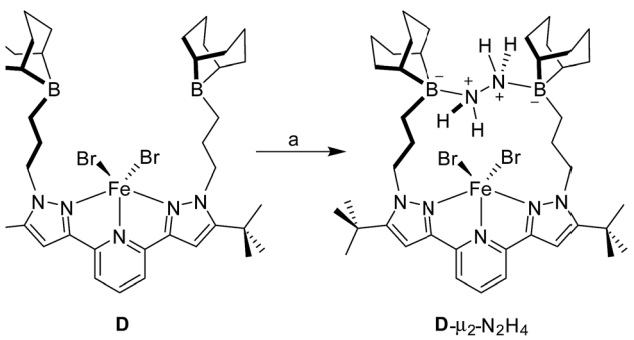


Fig. 5 The solid-state structure of **1**-μ_2-N_2H_4. Thermal ellipsoids are drawn at the 50% probability level. The hydrogen atoms, except that bound to the nitrogen atoms, are omitted for clarity. Selected bond lengths [Å] and angles [°]: B1–N1 1.688(2), N1–N1′ 1.469(2), B1–C1 1.627(21), B1–C7 1.651(2), B1–C16 1.647(2); B1–N1–N1′ 113.7(1), C7–B1–C16 118.7(1), C1–B1–C7 119.7(1), C1–B1–C16 106.6(1).



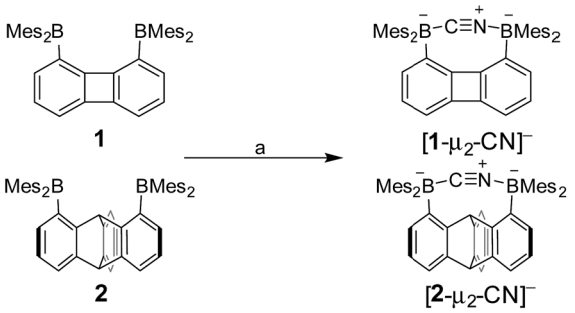
Scheme 3 Reaction of iron complex (**D**) with hydrazine to afford **D**-μ_2-N_2H_4 according to Szymczak *et al.* (a) 1 equiv. N_2H_4, THF, rt.

Reaction of the diboranes with the cyanide anion

Next in our survey of the properties of these diboranes, we decided to focus on the case of anions and especially the cyanide anion which is known for its acute toxicity and which has often been considered as a target in molecular recognition assays,[26] including using boron-based hosts.[17b,27]

Both diboranes quickly react with KCN in a CH_2Cl_2/MeOH (1/1 vol) mixture containing dibenzo-18-crown-6. As expected, this reaction is accompanied by a quenching of both the absorption and emission band (Fig. 4). In the case of **1**, these changes result in a distinct loss of both the yellow colour and the green fluorescence of the starting diborane (Fig. 4a). Workup of these reactions afforded the corresponding cyanide complexes [**1**-μ_2-CN]$^-$ and [**2**-μ_2-CN]$^-$ as air-stable [K(dibenzo-18-crown-6)]$^+$ salts (Scheme 4). The ^{11}B NMR signals detected for these anionic complexes (−15.8 ppm for [**1**-μ_2-CN]$^-$ and −11.7 ppm for [**2**-μ_2-CN]$^-$) are consistent with the existence of four-coordinate boron atoms. These signals are somewhat broad, possibly indicating the presence of two closely spaced and overlapping resonances corresponding to the N_{CN}-bound and C_{CN}-bound boron atoms, respectively. The presence of the cyanide anion in these complexes is confirmed by IR spectroscopy which shows that, in both cases, the cyanide stretching frequency (ν_{CN} = 2229 cm^{-1} for **1** and 2184 cm^{-1} for **2**) is higher than that of KCN (ν_{CN} = 2158 cm^{-1}). The higher energy of these vibrations is typical of cyanoborates. This effect can be rationalized by invoking a stabilization of the π molecular orbitals of the cyanide anion.[28] The absence of π-backbonding can also be invoked as a cause for this effect. The greater ν_{CN} observed for [**1**-μ_2-CN]$^-$ can be corroborated to the CV results and again suggest that the biphenylene backbone is more electron withdrawing than the triptycene backbone. The methyl region of the

Open Access Article. Published on 29 May 2018. Downloaded on 3/28/2024 8:53:24 AM.
This article is licensed under a Creative Commons Attribution-NonCommercial 3.0 Unported Licence.



Scheme 4 Synthesis of $[\mathbf{1}\text{-}\mu_2\text{-CN}]^-$ and $[\mathbf{2}\text{-}\mu_2\text{-CN}]^-$ as $[K(\text{dibenzo-18-crown-6})]^+$ salts. (a) 1 equiv. KCN, 1 equiv. dibenzo-18-crown-6, CH_2Cl_2/MeOH (1/1 vol), rt.

^{1}H NMR spectrum recorded for both $[\mathbf{1}\text{-}\mu_2\text{-CN}]^-$ and $[\mathbf{2}\text{-}\mu_2\text{-CN}]^-$ as $[K(\text{dibenzo-18-crown-6})]^+$ salts in $CDCl_3$ shows a level of complexity that is not consistent with equivalence of the two boryl moieties. We interpret these features as an evidence that the two boryl moieties are differentiated by their ligation to the C or N terminus of the cyanide anion.

Interestingly, diborane **1** and **2** appear to be highly selective for cyanide since no interaction with HCO_3^-, HSO_4^-, $H_2PO_4^-$, CH_3COO^-, Cl^-, Br^-, I^-, and N_3^- is observed in $CHCl_3$/MeOH (1/1 vol) by UV-vis spectrometry. Boranes are known to also display a large affinity for the fluoride anion. However, under these conditions, neither **1** nor **2** show any evidence of binding with fluoride. We propose that this selectivity is assisted by the specific architecture of the compounds that are well adapted to cyanide complexation (*vide infra*). However, considering that this selectivity could be biased by the protic nature of the medium which solvates the fluoride anion more effectively than the cyanide anion, we also tested the reaction with fluoride in dry $CDCl_3$. When **1** and **2** were combined with tetrabutylammonium difluorotriphenylsilicate (TBAT), no changes were observed in the ^{1}H NMR spectra of the diboranes indicating the absence of any interaction. When tetrabutylammonium fluoride trihydrate ($TBAF\cdot 3H_2O$) was used in dry $CDCl_3$, **1** underwent hydrolysis as previously described while **2** remained unperturbed.[12] Under the same conditions, both **1** and **2** quickly react with tetrabutylammonium cyanide (TBACN) to give the corresponding cyanide complexes. These results show that these diboranes are also selective for cyanide in organic solvents. Such selectivity is not unprecedented in the chemistry of boron-based Lewis acids.[17b,27] Lastly, these diboranes do not react with $LiHBEt_3$ in dry $CDCl_3$.

The structures of the cyanide complexes as $[K(\text{dibenzo-18-crown-6})]^+$ salts have been investigated by single crystal X-ray diffraction which confirms the μ(1,2) chelation of the cyanide anions (Fig. 6).[15] Both structures were solved on the basis of a model in which the cyanide anion is disordered over two overlapping head-to-tail positions, which as indicated by the refinements, contribute almost equally to the observed structures. In both structures, the boron atoms are distinctly pyramidal as indicated by the sum of the C_{aryl}–B–C_{aryl} angles which fall in the 341.7(4)–343.2(4)° range for $[\mathbf{1}\text{-}\mu_2\text{-CN}]^-$ and 342.0(5)–344.6(5)° for $[\mathbf{2}\text{-}\mu_2\text{-CN}]^-$. The accuracy of the crystallographic

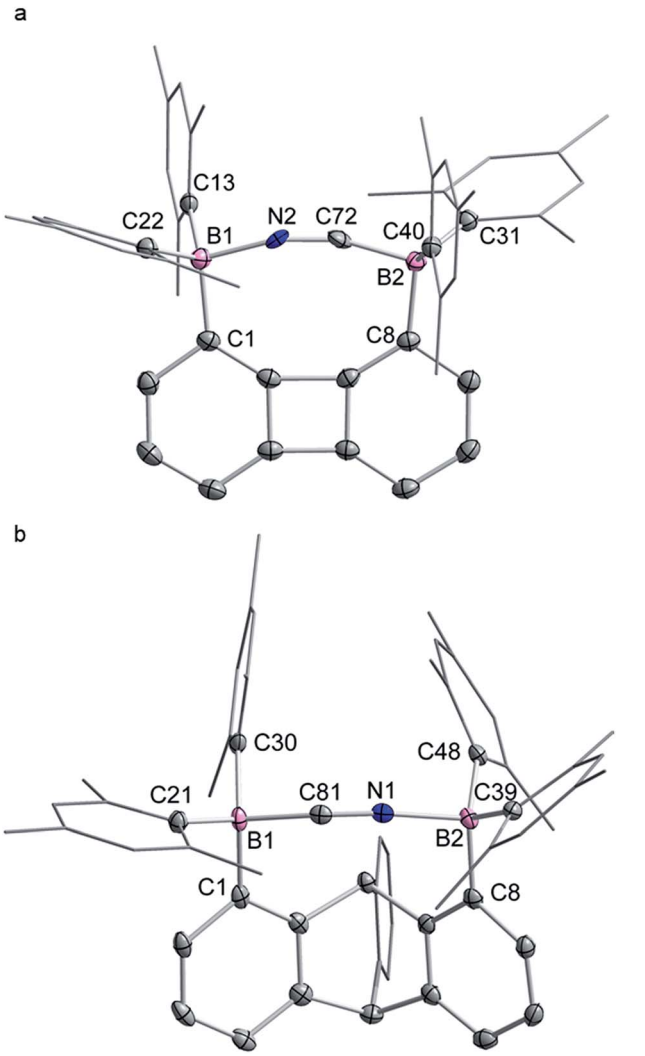


Fig. 6 Solid-state structures of the cyanide complexes $[K(\text{dibenzo-18-crown-6})][\mathbf{1}\text{-}\mu_2\text{-CN}]\text{-}(CH_2Cl_2)$ (a) and $[K(\text{dibenzo-18-crown-6})][\mathbf{2}\text{-}\mu_2\text{-CN}]\text{-}(CH_2Cl_2)_2$ (b). Thermal ellipsoids are drawn at the 50% probability level. The $[K(\text{dibenzo-18-crown-6})]^+$, the solvate molecules and the hydrogen atoms are omitted for clarity. The cyanide anions shown correspond to that with the higher positional occupancy. Selected bond lengths [Å] and angles [°] for $[\mathbf{1}\text{-}\mu_2\text{-CN}]^-$: B1–C1 1.635(4), B1–C13 1.649(4), B1–C22 1.639(4), B1–N2 1.58(2), B2–C8 1.641(4), B2–C31 1.643(4), B2–C40 1.657(3), B2–C72 1.54(4) C72–N2 1.21(4); C1–B1–C13 121.1(2), C13–B1–C22 113.8(2), C1–B1–C22 108.3(2), C1–B1–N2 100.9(7), C13–B1–N2 98.7(8), C22–B1–N2 112.9(7), B1–N2–C72 157.0(19), C8–B2–C31 108.4(2), C8–B2–C40 118.0(2), C31–B2–C40 115.3(2), C8–B2–C72 99.8(8), C31–B2–C72 115.8(9), C40–B2–C72 98.5(9), B2–C72–N2 163(2); for $[\mathbf{2}\text{-}\mu_2\text{-CN}]^-$: C1–B1 1.657(5), C21–B1 1.644(5), C30–B1 1.665(5), C81–B1 1.66(4), C81–N1 1.16(8), C8–B2 1.632(5), C39–B2 1.646(5), C48–B2 1.649(5), N1–B2 1.64(5); C1–B1–C21 109.1(3), C1–B1–C30 120.2(3), C21–B1–C30 112.7(3), C1–B1–C81 102.6(11), C21–B1–C81 111.4(16), C30–B1–C81 99.8(15), B1–C81–N1 158(6), C8–B2–C39 113.5(3), C8–B2–C48 113.1(3), C39–B2–C48 118.0(3), C8–B2–N1 99.8(15), C39–B2–N1 110.6(18), C48–B2–N1 99.1(13), B2–N1–C81 168(6).

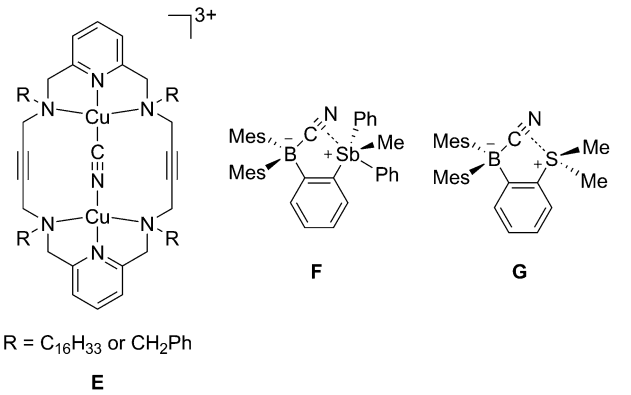
measurements does not allow for a comparison of the B–C_{CN} and B–N_{CN} bond distances which fall in the 1.54(4)–1.62(3) Å for $[\mathbf{1}\text{-}\mu_2\text{-CN}]^-$ and 1.63(5)–1.67(8) Å for $[\mathbf{2}\text{-}\mu_2\text{-CN}]^-$. The small difference in the B1–B2 separations in $[\mathbf{1}\text{-}\mu_2\text{-CN}]^-$ (4.187 (4) Å)

This journal is © The Royal Society of Chemistry 2018

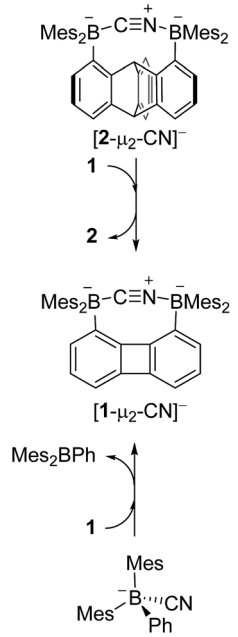
Open Access Article. Published on 29 May 2018. Downloaded on 3/28/2024 8:53:24 AM.
This article is licensed under a Creative Commons Attribution-NonCommercial 3.0 Unported Licence.

and **1** (4.566(5) Å) reflects the rigidity of the molecule. Compared to **1**, the large variation of the B1–B2 separation on going from **2** (B1–B2 5.559(4) Å) to [**2**-μ_2-CN]$^-$ (B1–B2 4.321(5) Å) speaks to the flexibility of the triptycene backbone and its pincer ability toward the cyanide anion. The behaviour of **1** and **2** and their ability to coordinate to both ends of the cyanide anion is reminiscent of the behaviour of dicopper(II) complexes (**E**) which also form μ(1,2) cyanide complexes as described by Krämer (Scheme 5).[29] This bonding mode differs from that observed for stibonium (**F**) and sulfonium boranes (**G**) in which the cyanide anion interact primarily with the boron atom, with a weak side on contact to the adjacent stibonium or sulfonium cation (Scheme 5).[27d,30] Finally, it is important to point out that while [**1**-μ_2-CN]$^-$ and [**2**-μ_2-CN]$^-$ are the first bimolecular μ(1,2) complexes formed by a diborane and cyanide, their cores are reminiscent of that found in termolecular complexes of general formula [Ar_3B–CN–BAr_3]$^-$ (Ar = Ph or C_6F_5).[31]

Since the CV data of **1** and **2** and the IR data of [**1**-μ_2-CN]$^-$ and [**2**-μ_2-CN]$^-$ suggest that **1** is a stronger Lewis acid than **2**, we became eager to experimentally confirm that **1** would indeed outcompete **2** with regard to cyanide binding. In accordance with this prediction, we observed, using ^{1}H NMR spectroscopy, the quantitative transfer of the cyanide anion from **2** to **1** when [^{n}Bu_4N][**2**-μ_2-CN] was mixed with an equimolar quantity of **1** in $CDCl_3/CD_3OD$ (1/1 vol) at 60 °C over the course of 12 h (Scheme 6). This observation confirms the higher cyanide ion affinity of **1** in protic solution, which is consistent with the electrochemical and IR measurements described above. Furthermore, a competition experiment was also performed with the monofunctional model borane Mes_2BPh (**3**). In these tests, the cyanide anion was transferred from [**3**-CN]$^-$ to **1** quantitatively in $CDCl_3/CD_3OD$ (1/1 vol) at 60 °C (Scheme 6). However, no transfer was observed between [**3**-CN]$^-$ and **2**. The absence of a reaction points to the weaker cyanide affinity of **2** when compared to **1**. The reversibility of the cyanide binding was also investigated by allowing [^{n}Bu_4N][**1**-μ_2-CN] and [^{n}Bu_4N][**2**-μ_2-CN] to react with one equivalent of $(C_6F_5)_3B$ in $CDCl_3/CD_3OD$ (1/1 vol).[32] Under these conditions, [**2**-μ_2-CN]$^-$ was readily converted into **2** while [**1**-μ_2-CN]$^-$ remained untouched, again supporting the superior Lewis acidity of **1**.



Scheme 5 Structure of the cyanide complexes of ditopic hosts E–G.



Scheme 6 Competition reactions of [^{n}Bu_4N][**2**-μ_2-CN] and **1** (top) and [^{n}Bu_4N][**3**-CN] and **1** (bottom). The [^{n}Bu_4N]$^+$ cations are not shown for clarity.

Conclusions

In summary, we describe two "large-bite" diboranes that are ideally suited for the selective μ(1,2) complexation of hydrazine and cyanide, two diatomic molecules that are known for their high toxicity. The high selectivity displayed for these two specific molecules highlights the defining role played by the backbone. The most potent binder is the biphenylene-based diborane which complexes both hydrazine and cyanide while the triptycene derivative only binds cyanide. A similar picture emerges from competition experiments which show that **1** is a better molecular recognition unit for cyanide than **2**. Our results and analyses indicate that the enhanced properties of **1** arise from the electron withdrawing nature of the biphenylene backbone. We also propose that the rigidity of this diborane is a favourable factor that helps sequester hydrazine and the cyanide anion in the diboron pocket. This binding appears to be irreversible in the case of the cyanide anion. In the case of the hydrazine complex, we observe that slow release can be triggered upon elevation of the temperature and in the presence of a reaction partner such as benzaldehyde. This last feature shows that such bidentate hosts could be used for the slow release of reactive compounds.

Experimental

Synthesis of 2

^{n}BuLi (2.65 M, 1 mL, 2.65 mmol) was slowly added to a solution of 1,8-dibromotriptycene (500 mg, 1.2 mmol) in dry THF (8 mL) under N_2 at −78 °C. After 30 min of stirring at low temperature, a solution of Mes_2BF (715 mg, 2.6 mmol) in THF (5 mL) was slowly transferred into the reaction flask using a cannula. The resulting solution was stirred for an additional 12 h at room

Open Access Article. Published on 29 May 2018. Downloaded on 3/28/2024 8:53:24 AM. This article is licensed under a Creative Commons Attribution-NonCommercial 3.0 Unported Licence.

temperature. The solution was then treated with saturated $NH_4Cl_{(aq)}$ (1 mL) and the solvent was removed under vacuum. The resulting white solid was then dissolved in CH_2Cl_2 (5 mL). The resulting solution was filtered and brought to dryness under vacuum. The off-white solid was then washed with MeOH (15 mL) twice and dried under vacuum to afford diborane **2** as a white powder in 60% yield. ^{1}H NMR (399.50 MHz, 25 °C, $CDCl_3$): δ 7.49 (d, 2H, $^3J_{H-H}$ = 6.6 Hz, triptycene-CH), 7.23 (d, 1H, $^3J_{H-H}$ = 7.0 Hz, triptycene-CH), 6.97 (pseudo t, 2H, $^3J_{H-H}$ = 7.4 Hz, triptycene-CH), 6.90–6.86 (m, 3H, triptycene-CH), 6.82 (s, 2H, mes-CH), 6.77 (s, 2H, mes-CH), 6.73 (s, 2H, mes-CH), 6.61 (pseudo t, 1H, $^3J_{H-H}$ = 7.4 Hz, triptycene-CH), 6.35 (s, 2H, mes-CH), 5.40 (s, 1H, triptycene-CH), 5.30 (d, 1H, $^3J_{H-H}$ = 7.4 Hz, triptycene-CH), 5.16 (s, 1H, triptycene-CH), 2.34 (s, 6H, –CH_3), 2.30 (s, 6H, –CH_3), 2.17 (s, 6H, –CH_3), 2.13 (s, 6H, –CH_3), 1.79 (s, 6H, –CH_3), 0.60 (s, 6H, –CH_3) ppm. ^{13}C NMR (100.46 MHz, 25 °C, $CDCl_3$): δ 150.86, 145.50, 145.23, 144.42, 144.27, 143.12, 141.52, 141.17, 140.90, 140.77, 139.89, 138.58, 138.57, 131.21, 129.92, 129.90, 128.47, 128.14, 127.90, 126.58, 126.17, 125.05, 124.16, 123.50, 121.60, 55.45 (triptycene-CH), 54.26 (triptycene-CH), 25.20 (–*C*H_3), 24.96 (–CH_3), 22.37 (–CH_3), 22.03 (–CH_3), 21.39 (–CH_3), 21.25 (–CH_3) ppm. ^{11}B (128.16 MHz, 25 °C, $CDCl_3$): δ 73.0 (br) ppm. Elemental analysis calculated (%) for $C_{56}H_{56}B_2$: C, 89.60; H, 7.52; found C, 89.62; H, 7.47.

Synthesis of 1-μ_2-N_2H_4

A solution of $N_2H_4\cdot H_2O$ (20 mg, 0.4 mmol) in THF (2 mL) was combined with a solution of diborane **1** (100 mg, 0.154 mmol) in THF (5 mL) at room temperature. The resulting solution was stirred for an additional hour and brought to dryness under vacuum. The resulting solid was washed twice with MeOH (5 mL) to afford **1**-μ_2-N_2H_4 as a off-white powder in 90% yield. ^{1}H NMR (499.48 MHz, 25 °C, CD_2Cl_2): δ 6.85 (s, 2H, mes-CH), 6.80 (s, 2H, mes-CH), 6.68 (s, 2H, mes-CH), 6.57 (s, 2H, mes-CH), 6.55–6.50 (m, 6H, biphenylene-CH), 6.31–6.28 (m, 2H, –NH_2–), 5.17–5.13 (m, 2H, –NH_2–), 2.25 (s, 6H, –CH_3), 2.24 (s, 6H, –CH_3), 2.15 (s, 6H, –CH_3), 1.80 (s, 6H, –CH_3), 1.74 (s, 6H, –CH_3), 1.67 (s, 6H, –CH_3) ppm. ^{13}C NMR (125.61 MHz, 25 °C, CD_2Cl_2): δ 151.26, 149.80, 143.94, 141.61, 139.50, 137.63, 137.42, 136.01, 135.58, 132.50, 131.24, 130.65, 130.60, 128.00, 115.17, 26.77(–CH_3), 25.72(–CH_3), 23.61(–CH_3), 23.21(–CH_3), 21.07(–CH_3), 20.87(–CH_3) ppm. ^{11}B (128.16 MHz, 25 °C, $CDCl_3$): not observed. Elemental analysis calculated (%) for $C_{48}H_{54}B_2N_2\cdot 0.93 \times CHCl_3$: C, 74.24; H, 6.99; found C, 74.22; H, 7.03. This EA result indicates the crystal sample obtain from $CHCl_3$/MeOH contains interstitial solvent molecules. This view is consistent with the crystallographic measurements which show the presence of disordered interstitial solvents equivalent to an electron count of 59 as indicated by application of the SQUEEZE protocol.[33] This electron count corresponds almost exactly to the number of electrons of a chloroform molecule (58). The EA results suggest partial loss of the interstitial chloroform molecule.

Synthesis of [K(dibenzo-18-crown-6)][1-μ_2-CN]

A solution of KCN (10 mg, 0.15 mmol) in MeOH (2 mL) was slowly added at room temperature into a CH_2Cl_2 solution (10 mL) containing **1** (100 mg, 0.15 mmol) and dibenzo-18-crown-6 (56 mg, 0.15 mmol). The resulting colourless solution was stirred for an additional 1 h at room temperature. The solvent was removed under vacuum and the resulting solid was washed by Et_2O (10 mL) twice to afford [K(dibenzo-18-crown-6)][**1**-μ_2-CN] as a white powder in 90% yield. ^{1}H NMR (499.53 MHz, 25 °C, $CDCl_3$): δ 7.00–6.97 (m, 4H, –C_6H_4–), 6.84–6.79 (m, 4H, –C_6H_4–), 6.66 (t, 2H, ^3J = 8.78 Hz, biphenylene-CH), 6.50 (br, 8H, mes-CH), 6.20–6.16 (m, 2H, biphenylene-CH), 6.10 (d, ^3J = 6.34 Hz, biphenylene-CH), 4.03–4.01 (m, 8H, –CH_2–), 3.76–3.74 (m, 8H, –CH_2–), 2.13 (br, 12H, –CH_3), 1.84 (br, 24H, –CH_3) ppm. ^{1}H NMR (399.46 MHz, −50 °C, $CDCl_3$): δ 6.95–6.94 (m, 4H, –C_6H_4–), 6.77–6.74 (m, 4H, –C_6H_4–), 6.67 (t, 2H, ^3J = 9.34 Hz, biphenylene-CH), 6.58–6.52 (m, 6H, mes-CH), 6.41 (s, 1H, mes-CH), 6.39 (s, 1H, mes-CH), 6.19–6.12 (m, 4H, biphenylene-CH), 3.94 (br, 8H, –CH_2–), 3.37 (br, 8H, –CH_2–), 2.18 (s, 6H, –CH_3), 2.14 (s, 3H, –CH_3), 2.11 (s, 3H, –CH_3), 2.05 (s, 6H, –CH_3), 1.84–1.80 (m, 12H, –CH_3), 1.70 (s, 6H, –CH_3) ppm. ^{13}C NMR (125.62 MHz, 25 °C, $CDCl_3$): δ 158.33, 157.36, 150.05, 146.14, 137.01, 136.28, 132.48, 132.37, 128.55, 124.36, 122.25, 112.02, 111.77, 80.29, 68.97 (–CH_2–), 66.59 (–CH_2–), 24.44 (–CH_3), 20.82 (–CH_3) ppm. ^{11}B (128.16 MHz, 25 °C, $CDCl_3$): δ −15.8 ppm. IR ν_{CN} = 2229 cm^{-1}. Elemental analysis calculated (%) for $C_{69}H_{74}B_2KO_6\cdot 0.55 \times CH_2Cl_2$: C, 75.48; H, 6.84; found C, 75.49; H, 6.78. These EA results indicate partial loss of the interstitial solvent molecules.

Synthesis of [K(dibenzo-18-crown-6)][2-μ_2-CN]

A solution of KCN (10 mg, 0.15 mmol) in MeOH (2 mL) was slowly added at room temperature into a CH_2Cl_2 solution (10 mL) containing **2** (116 mg, 0.15 mmol) and dibenzo-18-crown-6 (56 mg, 0.15 mmol). The resulting colourless solution was stirred for an additional 1 h at room temperature. The solvent was removed under vacuum and the resulting solid was washed by Et_2O (10 mL) twice to afford [K(dibenzo-18-crown-6)][**2**-μ_2-CN] as a white powder in 88% yield. ^{1}H NMR (499.49 MHz, 25 °C, CD_2Cl_2): δ 7.32 (d, 1H, $^3J_{H-H}$ = 7.3 Hz, triptycene-CH), 7.09 (d, 2H, $^3J_{H-H}$ = 7.3 Hz, triptycene-CH), 7.04–6.98 (m, 5H), 6.93–6.88 (m, 6H), 6.84 (d, 1H, $^3J_{H-H}$ = 7.3 Hz, triptycene-CH), 6.66 (s, 2H, mes-CH), 6.58 (pseudo t, 2H, $^3J_{H-H}$ = 7.3 Hz, triptycene-CH), 6.53 (s, 1H, mes-CH), 6.52 (s, 2H, mes-CH), 6.48 (s, 1H, mes-CH), 6.41 (d, 1H, $^3J_{H-H}$ = 7.8 Hz, triptycene-CH), 6.37 (d, 1H, $^3J_{H-H}$ = 7.8 Hz, triptycene-CH), 6.31 (s, 1H, mes-CH), 6.27 (s, 1H, mes-CH), 5.74 (s, 1H, triptycene-CH), 5.26 (s, 1H, triptycene-CH), 4.18–4.16 (m, 8H, –CH_2–), 3.93–3.91 (m, 8H, –CH_2–), 2.25 (s, 3H, –CH_3), 2.23 (s, 3H, –CH_3), 2.19 (s, 6H, –CH_3), 2.14 (s, 3H, –CH_3), 2.02 (s, 3H, –CH_3), 2.00 (s, 3H, –CH_3), 1.95 (s, 3H, –CH_3), 1.63 (s, 3H, –CH_3), 1.62 (s, 3H, –CH_3), 1.18 (s, 3H, –CH_3), 1.13 (s, 3H, –CH_3) ppm. ^{13}C NMR (125.61 MHz, 25 °C, CD_2Cl_2): δ 151.30, 150.72, 147.52, 146.65, 146.59, 144.42, 144.27, 143.19, 142.76, 142.53, 142.21, 141.89, 141.66, 140.88, 133.17, 130.01, 132.75, 132.63, 131.47, 131.34, 129.29, 129.12, 129.02, 128.90, 128.73, 128.60, 128.15, 126.69, 124.49, 123.46, 122.85, 122.57, 122.48, 121.56, 120.50, 120.40, 111.95, 69.85 (–CH_2–), 67.21 (–CH_2–), 56.15 (triptycene-CH), 51.86 (triptycene-CH), 26.87 (–CH_3), 25.97 (–CH_3), 25.91 (–CH_3), 25.77 (–CH_3), 25.55

 This journal is © The Royal Society of Chemistry 2018

Open Access Article. Published on 29 May 2018. Downloaded on 3/28/2024 8:53:24 AM.
This article is licensed under a Creative Commons Attribution-NonCommercial 3.0 Unported Licence.

(–CH_3), 25.48 (–CH_3), 24.79 (–CH_3), 24.48 (–CH_3), 21.24 (–CH_3), 20.86 (–CH_3) ppm. ^{11}B (128.16 MHz, 25 °C, $CDCl_3$): δ −11.7 ppm. IR $\nu_{CN} = 2184\ cm^{-1}$. Elemental analysis calculated (%) for $C_{77}H_{80}B_2KNO_6 \cdot 0.43 \times CH_2Cl_2$: C, 76.69; H, 6.72; found C, 76.70; H, 6.71. These EA results indicate partial loss of the interstitial solvent molecules.

Computational details

Density functional theory (DFT) structural optimizations of **1** and **2** were carried with the Gaussian 09 program. In all cases, the structures were optimized using the B3LYP functional and the following mixed basis set: C/H, 6-31g; B, 6-31g+(d′). For all optimized structures, frequency calculations were carried out to confirm the absence of imaginary frequencies. The molecular orbitals were visualized and plotted using the Jimp2 program. The TD-DFT and NTO calculations were carried out using the MPW1PW91 functional and the above-mentioned basis sets.

Conflicts of interest

The authors declare no conflict of interest.

Acknowledgements

Acknowledgment is made to the donors of the American Chemical Society Petroleum Research Fund for partial support of this research (Grant 56871-ND3). We also acknowledge support from the Welch Foundation (Grant A-1423), Texas A&M University (Arthur E. Martell Chair of Chemistry), and the Laboratory for Molecular Simulation at Texas A&M University (software and computational resources) is gratefully acknowledged.

References

1 (*a*) T. W. Hudnall, C.-W. Chiu and F. P. Gabbaï, *Acc. Chem. Res.*, 2009, **42**, 388–397; (*b*) E. Galbraith and T. D. James, *Chem. Soc. Rev.*, 2010, **39**, 3831–3842; (*c*) C. R. Wade, A. E. J. Broomsgrove, S. Aldridge and F. P. Gabbaï, *Chem. Rev.*, 2010, **110**, 3958–3984; (*d*) *Anion Coordination Chemistry*, ed., K. Bowman-James, A. Bianchi and E. Garcia-Espana, Wiley-VCH Verlag GmbH & Co. KGaA, 2012; (*e*) H. Zhao, L. A. Leamer and F. P. Gabbaï, *Dalton Trans.*, 2013, **42**, 8164–8178; (*f*) N. Busschaert, C. Caltagirone, W. Van Rossom and P. A. Gale, *Chem. Rev.*, 2015, **115**, 8038–8155; (*g*) P. A. Gale, E. N. W. Howe, X. Wu and M. J. Spooner, *Coord. Chem. Rev.*, 2018, DOI: 10.1016/j.ccr.2018.02.005.

2 (*a*) M. H. Lee and F. P. Gabbaï, *Inorg. Chem.*, 2007, **46**, 8132–8138; (*b*) J. K. Day, C. Bresner, N. D. Coombs, I. A. Fallis, L.-L. Ooi and S. Aldridge, *Inorg. Chem.*, 2008, **47**, 793–804; (*c*) P. Chen and F. Jäkle, *J. Am. Chem. Soc.*, 2011, **133**, 20142–20145; (*d*) P. Chen, A. S. Marshall, S.-H. Chi, X. Yin, J. W. Perry and F. Jäkle, *Chem.–Eur. J.*, 2015, **21**, 18237–18247; (*e*) M. Hirai and F. P. Gabbaï, *Angew. Chem., Int. Ed.*, 2015, **54**, 1205–1209.

3 (*a*) M. E. Jung and H. Xia, *Tetrahedron Lett.*, 1988, **29**, 297–300; (*b*) M. Rothmaier and W. Simon, *Anal. Chim. Acta*, 1993, **271**, 135–141; (*c*) I. H. A. Badr, M. Diaz, M. F. Hawthorne and L. G. Bachas, *Anal. Chem.*, 1999, **71**, 1371–1377; (*d*) N. Chaniotakis, K. Jurkschat, D. Mueller, K. Perdikaki and G. Reeske, *Eur. J. Inorg. Chem.*, 2004, 2283–2288; (*e*) Z. Yan, Z. Zhou, Y. Wu, I. A. Tikhonova and V. B. Shur, *Anal. Lett.*, 2005, **38**, 377–388; (*f*) A. V. Jentzsch, D. Emery, J. Mareda, S. K. Nayak, P. Metrangolo, G. Resnati, N. Sakai and S. Matile, *Nat. Commun.*, 2012, **3**, 905; (*g*) S. Benz, M. Macchione, Q. Verolet, J. Mareda, N. Sakai and S. Matile, *J. Am. Chem. Soc.*, 2016, **138**, 9093–9096.

4 (*a*) S. H. Jungbauer and S. M. Huber, *J. Am. Chem. Soc.*, 2015, **137**, 12110–12120; (*b*) M. H. Holthausen, J. M. Bayne, I. Mallov, R. Dobrovetsky and D. W. Stephan, *J. Am. Chem. Soc.*, 2015, **137**, 7298–7301; (*c*) M. Hirai, J. Cho and F. P. Gabbaï, *Chem.–Eur. J.*, 2016, **22**, 6537–6541; (*d*) S. Benz, J. López-Andarias, J. Mareda, N. Sakai and S. Matile, *Angew. Chem., Int. Ed.*, 2017, **56**, 812–815; (*e*) L. Wang, S. Zhang, Y. Hasegawa, C. G. Daniliuc, G. Kehr and G. Erker, *Chem. Commun.*, 2017, **53**, 5499–5502; (*f*) S. Benz, J. Mareda, C. Besnard, N. Sakai and S. Matile, *Chem. Sci.*, 2017, **8**, 8164–8169; (*g*) D. Chen, G. Xu, Q. Zhou, L. W. Chung and W. Tang, *J. Am. Chem. Soc.*, 2017, **139**, 9767–9770.

5 (*a*) H. E. Katz, *J. Org. Chem.*, 1985, **50**, 5027–5032; (*b*) H. E. Katz, *J. Am. Chem. Soc.*, 1985, **107**, 1420–1421; (*c*) H. E. Katz, *Organometallics*, 1987, **6**, 1134–1136; (*d*) M. Reilly and T. Oh, *Tetrahedron Lett.*, 1994, **35**, 7209–7212; (*e*) M. Melaïmi, S. Sole, C.-W. Chiu, H. Wang and F. P. Gabbaï, *Inorg. Chem.*, 2006, **45**, 8136–8143; (*f*) C. Jiang, O. Blacque and H. Berke, *Chem. Commun.*, 2009, 5518–5520; (*g*) H. Zhao and F. P. Gabbaï, *Organometallics*, 2012, **31**, 2327–2335.

6 (*a*) V. C. Williams, W. E. Piers, W. Clegg, M. R. J. Elsegood, S. Collins and T. B. Marder, *J. Am. Chem. Soc.*, 1999, **121**, 3244–3245; (*b*) S. P. Lewis, N. J. Taylor, W. E. Piers and S. Collins, *J. Am. Chem. Soc.*, 2003, **125**, 14686–14687; (*c*) J. Chai, S. P. Lewis, S. Collins, T. J. J. Sciarone, L. D. Henderson, P. A. Chase, G. J. Irvine, W. E. Piers, M. R. J. Elsegood and W. Clegg, *Organometallics*, 2007, **26**, 5667–5679; (*d*) L. D. Henderson and W. E. Piers, *J. Organomet. Chem.*, 2007, **692**, 4661–4668; (*e*) M. V. Metz, D. J. Schwartz, C. L. Stern, P. N. Nickias and T. J. Marks, *Angew. Chem., Int. Ed.*, 2000, **39**, 1312–1316; (*f*) V. C. Williams, G. J. Irvine, W. E. Piers, Z. Li, S. Collins, W. Clegg, M. R. J. Elsegood and T. B. Marder, *Organometallics*, 2000, **19**, 1619–1621; (*g*) S. N. Kessler, M. Neuburger and H. A. Wegner, *J. Am. Chem. Soc.*, 2012, **134**, 17885–17888; (*h*) E. von Grotthuss, M. Diefenbach, M. Bolte, H.-W. Lerner, M. C. Holthausen and M. Wagner, *Angew. Chem., Int. Ed.*, 2016, **55**, 14067–14071; (*i*) J. W. Taylor, A. McSkimming, C. F. Guzman and W. H. Harman, *J. Am. Chem. Soc.*, 2017, **139**, 11032–11035.

7 A. Lorbach, M. Bolte, H.-W. Lerner and M. Wagner, *Chem. Commun.*, 2010, **46**, 3592–3594.

Open Access Article. Published on 29 May 2018. Downloaded on 3/28/2024 8:53:24 AM. This article is licensed under a Creative Commons Attribution-NonCommercial 3.0 Unported Licence.

8 (*a*) S. N. Kessler, M. Neuburger and H. A. Wegner, *Eur. J. Org. Chem.*, 2011, **2011**, 3238–3245; (*b*) L. Schweighauser and H. A. Wegner, *Chem.–Eur. J.*, 2016, **22**, 14094–14103.

9 D. J. H. Emslie, W. E. Piers and M. Parvez, *Angew. Chem., Int. Ed.*, 2003, **42**, 1252–1255.

10 (*a*) H. E. Katz, *J. Org. Chem.*, 1989, **54**, 2179–2183; (*b*) H. Wang and F. P. Gabbaï, *Organometallics*, 2005, **24**, 2898–2902; (*c*) J. J. Kiernicki, M. Zeller and N. K. Szymczak, *J. Am. Chem. Soc.*, 2017, **139**, 18194–18197.

11 (*a*) N. Lopez, D. J. Graham, R. McGuire, G. E. Alliger, Y. Shao-Horn, C. C. Cummins and D. G. Nocera, *Science*, 2012, **335**, 450–453; (*b*) M. Nava, N. Lopez, P. Müller, G. Wu, D. G. Nocera and C. C. Cummins, *J. Am. Chem. Soc.*, 2015, **137**, 14562–14565; (*c*) E. W. Dahl, H. T. Dong and N. K. Szymczak, *Chem. Commun.*, 2018, **54**, 892–895.

12 C.-H. Chen and F. P. Gabbaï, *Angew. Chem., Int. Ed.*, 2018, **57**, 521–525.

13 S. Kirschner, J.-M. Mewes, M. Bolte, H.-W. Lerner, A. Dreuw and M. Wagner, *Chem.–Eur. J.*, 2017, **23**, 5104–5116.

14 (*a*) J. D. Hoefelmeyer and F. P. Gabbaï, *J. Am. Chem. Soc.*, 2000, **122**, 9054–9055; (*b*) J. D. Hoefelmeyer, S. Solé and F. P. Gabbaï, *Dalton Trans.*, 2004, 1254–1258.

15 CCDC 1838442 (**1**-μ_2-N_2H_4), 1827003 (**2**), 1827004 ([K(dibenzo-18-crown-6)][**1**-μ_2-CN]-(CH_2Cl_2)) and 1827005 ([K(dibenzo-18-crown-6)][**2**-μ_2-CN]-(CH_2Cl_2)$_2$) contain the supplementary crystallographic data for this paper.†

16 (*a*) K. Parab, K. Venkatasubbaiah and F. Jäkle, *J. Am. Chem. Soc.*, 2006, **128**, 12879–12885; (*b*) S. Yamaguchi and A. Wakamiya, *Pure Appl. Chem.*, 2006, **78**, 1413–1424; (*c*) Z. M. Hudson and S. Wang, *Acc. Chem. Res.*, 2009, **42**, 1584–1596; (*d*) H. Y. Zhao and F. P. Gabbai, *Nat. Chem.*, 2010, **2**, 984–990; (*e*) A. L. Brazeau, K. Yuan, S.-B. Ko, I. Wyman and S. Wang, *ACS Omega*, 2017, **2**, 8625–8632.

17 (*a*) S. Yamaguchi, S. Akiyama and K. Tamao, *J. Am. Chem. Soc.*, 2001, **123**, 11372–11375; (*b*) T. Matsumoto, C. R. Wade and F. P. Gabbaï, *Organometallics*, 2010, **29**, 5490–5495; (*c*) K. C. Song, K. M. Lee, N. V. Nghia, W. Y. Sung, Y. Do and M. H. Lee, *Organometallics*, 2013, **32**, 817–823.

18 (*a*) S. Pylypko, E. Petit, P. G. Yot, F. Salles, M. Cretin, P. Miele and U. B. Demirci, *Inorg. Chem.*, 2015, **54**, 4574–4583; (*b*) G. Qi, K. Wang, K. Yang and B. Zou, *J. Phys. Chem. C*, 2016, **120**, 21293–21298.

19 (*a*) Y. Yu, W. W. Brennessel and P. L. Holland, *Organometallics*, 2007, **26**, 3217–3226; (*b*) Y. Lee, N. P. Mankad and J. C. Peters, *Nat. Chem.*, 2010, **2**, 558; (*c*) C. T. Saouma, C. C. Lu and J. C. Peters, *Inorg. Chem.*, 2012, **51**, 10043–10054; (*d*) K. Umehara, S. Kuwata and T. Ikariya, *J. Am. Chem. Soc.*, 2013, **135**, 6754–6757; (*e*) Y. Li, Y. Li, B. Wang, Y. Luo, D. Yang, P. Tong, J. Zhao, L. Luo, Y. Zhou, S. Chen, F. Cheng and J. Qu, *Nat. Chem.*, 2013, **5**, 320.

20 B. Roy and S. Bandyopadhyay, *Anal. Methods*, 2018, **10**, 1117–1139.

21 (*a*) J. T. Henthorn and T. Agapie, *Angew. Chem., Int. Ed.*, 2014, **53**, 12893–12896; (*b*) X. Tao, C. G. Daniliuc, O. Janka, R. Pöttgen, R. Knitsch, M. R. Hansen, H. Eckert, M. Lübbesmeyer, A. Studer, G. Kehr and G. Erker, *Angew. Chem., Int. Ed.*, 2017, **56**, 16641–16644.

22 C.-H. Chen and F. P. Gabbaï, *Angew. Chem., Int. Ed.*, 2017, **56**, 1799–1804.

23 S. Mebs, S. Grabowsky, D. Förster, R. Kickbusch, M. Hartl, L. L. Daemen, W. Morgenroth, P. Luger, B. Paulus and D. Lentz, *J. Phys. Chem. A*, 2010, **114**, 10185–10196.

24 K. Kohata, T. Fukuyama and K. Kuchitsu, *J. Phys. Chem.*, 1982, **86**, 602–606.

25 E. Leusmann, F. Schneck and S. Dehnen, *Organometallics*, 2015, **34**, 3264–3271.

26 (*a*) Z. Xu, X. Chen, H. N. Kim and J. Yoon, *Chem. Soc. Rev.*, 2010, **39**, 127–137; (*b*) Z. Liu, W. He and Z. Guo, *Chem. Soc. Rev.*, 2013, **42**, 1568–1600; (*c*) F. Wang, L. Wang, X. Chen and J. Yoon, *Chem. Soc. Rev.*, 2014, **43**, 4312–4324; (*d*) T. D. Ashton, K. A. Jolliffe and F. M. Pfeffer, *Chem. Soc. Rev.*, 2015, **44**, 4547–4595.

27 (*a*) T. W. Hudnall and F. P. Gabbaï, *J. Am. Chem. Soc.*, 2007, **129**, 11978–11986; (*b*) C.-W. Chiu and F. P. Gabbaï, *Dalton Trans.*, 2008, 814–817; (*c*) C.-W. Chiu, Y. Kim and F. P. Gabbaï, *J. Am. Chem. Soc.*, 2009, **131**, 60–61; (*d*) Y. Kim, H. Zhao and F. P. Gabbaï, *Angew. Chem., Int. Ed.*, 2009, **48**, 4957–4960; (*e*) A. E. J. Broomsgrove, D. A. Addy, A. Di Paolo, I. R. Morgan, C. Bresner, V. Chislett, I. A. Fallis, A. L. Thompson, D. Vidovic and S. Aldridge, *Inorg. Chem.*, 2010, **49**, 157–173; (*f*) C. R. Wade and F. P. Gabbaï, *Inorg. Chem.*, 2010, **49**, 714–720; (*g*) Y. Kim, H.-S. Huh, M. H. Lee, I. L. Lenov, H. Zhao and F. P. Gabbaï, *Chem.–Eur. J.*, 2011, **17**, 2057–2062.

28 D. F. Shriver and J. Posner, *J. Am. Chem. Soc.*, 1966, **88**, 1672–1677.

29 (*a*) B. Ahlers, K. Cammann, S. Warzeska and R. Krämer, *Angew. Chem., Int. Ed.*, 1996, **35**, 2141–2143; (*b*) S. Warzeska and R. Krämer, *Chem. Commun.*, 1996, 499–500.

30 C. R. Wade and F. P. Gabbaï, *Z. Naturforsch., B: J. Chem. Sci.*, 2014, **69**, 1199–1205.

31 (*a*) C. M. Giandomenico, J. C. Dewan and S. J. Lippard, *J. Am. Chem. Soc.*, 1981, **103**, 1407–1412; (*b*) S. J. Lancaster, D. A. Walker, M. Thornton-Pett and M. Bochmann, *Chem. Commun.*, 1999, 1533–1534; (*c*) J. Zhou, S. J. Lancaster, D. A. Walker, S. Beck, M. Thornton-Pett and M. Bochmann, *J. Am. Chem. Soc.*, 2001, **123**, 223–237; (*d*) N. M. Brunkan, D. M. Brestensky and W. D. Jones, *J. Am. Chem. Soc.*, 2004, **126**, 3627–3641.

32 C. Bergquist, B. M. Bridgewater, C. J. Harlan, J. R. Norton, R. A. Friesner and G. Parkin, *J. Am. Chem. Soc.*, 2000, **122**, 10581–10590.

33 A. Spek, *Acta Crystallogr., Sect. C: Struct. Chem.*, 2015, **71**, 9–18.

 This journal is © The Royal Society of Chemistry 2018